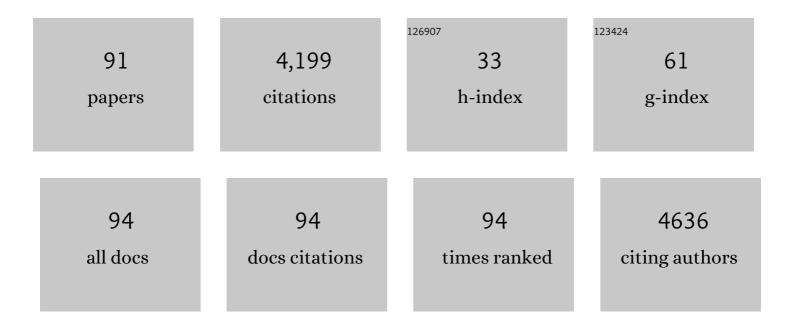
## Xiangzhong Ren

List of Publications by Year in descending order

Source: https://exaly.com/author-pdf/3926395/publications.pdf Version: 2024-02-01



#	Article	IF	CITATIONS
1	A Multiscale Strategy to Construct Cobalt Nanoparticles Confined within Hierarchical Carbon Nanofibers for Efficient CO <sub>2</sub> Electroreduction. Small, 2022, 18, e2104958.	10.0	4
2	Efficient capture and conversion of polysulfides by zinc protoporphyrin framework-embedded triple-layer nanofiber separator for advanced Li-S batteries. Journal of Colloid and Interface Science, 2022, 609, 43-53.	9.4	9
3	Construction of single-atom copper sites with low coordination number for efficient CO <sub>2</sub> electroreduction to CH <sub>4</sub> . Journal of Materials Chemistry A, 2022, 10, 6187-6192.	10.3	24
4	Deeply self-reconstructing CoFe(H3O)(PO4)2 to low-crystalline Fe0.5Co0.5OOH with Fe3+–O–Fe3+ motifs for oxygen evolution reaction. Applied Catalysis B: Environmental, 2022, 304, 120986.	20.2	36
5	Supramolecular Adhesive Hydrogels for Tissue Engineering Applications. Chemical Reviews, 2022, 122, 5604-5640.	47.7	238
6	Elucidating the activity, mechanism and application of selective electrosynthesis of ammonia from nitrate on cobalt phosphide. Energy and Environmental Science, 2022, 15, 760-770.	30.8	133
7	MoS <sub>2</sub> nanosheets vertically grown on CoSe <sub>2</sub> hollow nanotube arrays as an efficient catalyst for the hydrogen evolution reaction. Nanoscale, 2022, 14, 2490-2501.	5.6	18
8	Rational design of Ru species on N-doped graphene promoting water dissociation for boosting hydrogen evolution reaction. Science China Chemistry, 2022, 65, 521-531.	8.2	12
9	Tumor Microenvironment Activated Chemodynamic–Photodynamic Therapy by Multistage Selfâ€Assembly Engineered Protein Nanomedicine. Advanced Functional Materials, 2022, 32, .	14.9	15
10	Band Engineering Induced Conducting 2Hâ€Phase MoS <sub>2</sub> by PdSRe Sites Modification for Hydrogen Evolution Reaction. Advanced Energy Materials, 2022, 12, .	19.5	37
11	In-Plane Charge Transport Dominates the Overall Charge Separation and Photocatalytic Activity in Crystalline Carbon Nitride. ACS Catalysis, 2022, 12, 4648-4658.	11.2	69
12	Breaking the Limitation of Elevated Coulomb Interaction in Crystalline Carbon Nitride for Visible and Nearâ€Infrared Light Photoactivity. Advanced Science, 2022, 9, .	11.2	22
13	Defective Fe <sub>3</sub> O <sub>4â€</sub> <i><sub>x</sub></i> Fewâ€Atom Clusters Anchored on Nitrogenâ€Doped Carbon as Efficient Oxygen Reduction Electrocatalysts for Highâ€Performance Zinc–Air Batteries. Small Methods, 2022, 6, .	8.6	10
14	Double-Enhanced Core–Shell–Shell Sb <sub>2</sub> S <sub>3</sub> /Sb@TiO <sub>2</sub> @C Nanorod Composites for Lithium- and Sodium-Ion Batteries. ACS Applied Materials & Interfaces, 2022, 14, 33064-33075.	8.0	15
15	Ultrathin MoS2 anchored on 3D carbon skeleton containing SnS quantum dots as a high-performance anode for advanced lithium ion batteries. Chemical Engineering Journal, 2021, 403, 126251.	12.7	105
16	Amorphous MoS3 decoration on 2D functionalized MXene as a bifunctional electrode for stable and robust lithium storage. Chemical Engineering Journal, 2021, 406, 126775.	12.7	59
17	Engineering defect-rich Fe-doped NiO coupled Ni cluster nanotube arrays with excellent oxygen evolution activity. Applied Catalysis B: Environmental, 2021, 285, 119809.	20.2	103
18	Construction of cobalt oxyhydroxide nanosheets with rich oxygen vacancies as high-performance lithium-ion battery anodes. Journal of Materials Chemistry A, 2021, 9, 453-462.	10.3	47

XIANGZHONG REN

#	Article	IF	CITATIONS
19	Co–Mo–P carbon nanospheres derived from metal–organic frameworks as a high-performance electrocatalyst towards efficient water splitting. Journal of Materials Chemistry A, 2021, 9, 1143-1149.	10.3	36
20	Heterostructure enhanced sodium storage performance for SnS <sub>2</sub> in hierarchical SnS <sub>2</sub> /Co <sub>3</sub> S <sub>4</sub> nanosheet array composite. Journal of Materials Chemistry A, 2021, 9, 1630-1642.	10.3	30
21	Extraordinary dual-ion electrochemical deionization capacity and energy efficiency enabled by coupling of Na <sub>3</sub> Fe <sub>2</sub> (PO <sub>4</sub> ) <sub>3</sub> and NiVAl layered double hydroxide electrodes. Journal of Materials Chemistry A, 2021, 9, 22913-22925.	10.3	9
22	<i>In situ</i> formed lithium ionic conductor thin film on the surface of high-crystal-layered LiCoO <sub>2</sub> as a high-voltage cathode material. Materials Chemistry Frontiers, 2021, 5, 6171-6181.	5.9	8
23	Carbon nanotubes coupled with layered graphite to support SnTe nanodots as high-rate and ultra-stable lithium-ion battery anodes. Nanoscale, 2021, 13, 3782-3789.	5.6	23
24	Long cyclic stability of acidic aqueous zinc-ion batteries achieved by atomic layer deposition: the effect of the induced orientation growth of the Zn anode. Nanoscale, 2021, 13, 12223-12232.	5.6	33
25	Recent Progress in 2D Catalysts for Photocatalytic and Electrocatalytic Artificial Nitrogen Reduction to Ammonia. Advanced Energy Materials, 2021, 11, 2003294.	19.5	73
26	Synthesis of V-notched half-open polymer microspheres <i>via</i> facile solvent-tuned self-assembly. New Journal of Chemistry, 2021, 45, 13964-13968.	2.8	1
27	Confining Sb <sub>2</sub> Se <sub>3</sub> nanorod yolk in a mesoporous carbon shell with an in-built buffer space for stable Li-ion batteries. Journal of Materials Chemistry A, 2021, 9, 3388-3397.	10.3	35
28	2D Electrocatalysts: Recent Progress in 2D Catalysts for Photocatalytic and Electrocatalytic Artificial Nitrogen Reduction to Ammonia (Adv. Energy Mater. 11/2021). Advanced Energy Materials, 2021, 11, 2170043.	19.5	3
29	An Insightful Picture of Nonlinear Photonics in 2DÂMaterials and their Applications: Recent Advances and Future Prospects. Advanced Optical Materials, 2021, 9, 2001671.	7.3	23
30	Engineering hollow multi-shelled Co3O4 cubes to boost lithium storage performance. Applied Surface Science, 2021, 545, 149022.	6.1	9
31	Protein-Based Nanomedicine for Therapeutic Benefits of Cancer. ACS Nano, 2021, 15, 8001-8038.	14.6	59
32	Electrochemical Construction of Low-Crystalline CoOOH Nanosheets with Short-Range Ordered Grains to Improve Oxygen Evolution Activity. ACS Catalysis, 2021, 11, 6104-6112.	11.2	103
33	Construction of K <sup>+</sup> Ion Gradient in Crystalline Carbon Nitride to Accelerate Exciton Dissociation and Charge Separation for Visible Light H <sub>2</sub> Production. ACS Catalysis, 2021, 11, 6995-7005.	11.2	100
34	Ultraâ€lowâ€loaded Niâ^'Fe Dimer Anchored to Nitrogen/Oxygen Sites for Boosting Electroreduction of Carbon Dioxide. ChemSusChem, 2021, 14, 4499-4506.	6.8	9
35	Multiple anionic Ni(SO4)0.3(OH)1.4 nanobelts/reduced graphene oxide enabled by enhanced multielectron reactions with superior lithium storage capacity. Chemical Engineering Journal, 2021, 426, 131863.	12.7	3
36	Tuning and understanding the electronic effect of Co–Mo–O sites in bifunctional electrocatalysts for ultralong-lasting rechargeable zinc–air batteries. Journal of Materials Chemistry A, 2021, 9, 21716-21722.	10.3	16

#	Article	IF	CITATIONS
37	ZIF-derived "senbei―like Co <sub>9</sub> S <sub>8</sub> /CeO <sub>2</sub> /Co heterostructural nitrogen-doped carbon nanosheets as bifunctional oxygen electrocatalysts for Zn-air batteries. Nanoscale, 2021, 13, 3227-3236.	5.6	33
38	Bifunctional oxygen electrocatalysis on ultra-thin Co <sub>9</sub> S <sub>8</sub> /MnS carbon nanosheets for all-solid-state zinc–air batteries. Journal of Materials Chemistry A, 2021, 9, 22635-22642.	10.3	22
39	Rapid ionic conductivity of ternary composite electrolytes for superior solid-state batteries with high-rate performance and long cycle life operated at room temperature. Journal of Materials Chemistry A, 2021, 9, 18338-18348.	10.3	23
40	Unveiling the reaction mechanism of an Sb <sub>2</sub> S <sub>3</sub> –Co <sub>9</sub> S <sub>8</sub> /NC anode for high-performance lithium-ion batteries. Nanoscale, 2021, 13, 20041-20051.	5.6	13
41	Unconventionally fabricating defect-rich NiO nanoparticles within ultrathin metal–organic framework nanosheets to enable high-output oxygen evolution. Journal of Materials Chemistry A, 2020, 8, 2140-2146.	10.3	66
42	One-pot synthesis of N,S-doped pearl chain tube-loaded Ni3S2 composite materials for high-performance lithium–air batteries. Nanoscale, 2020, 12, 21770-21779.	5.6	7
43	A unique space confined strategy to construct defective metal oxides within porous nanofibers for electrocatalysis. Energy and Environmental Science, 2020, 13, 5097-5103.	30.8	80
44	Co/CoP Nanoparticles Encapsulated Within N, P-Doped Carbon Nanotubes on Nanoporous Metal-Organic Framework Nanosheets for Oxygen Reduction and Oxygen Evolution Reactions. Nanoscale Research Letters, 2020, 15, 82.	5.7	20
45	Sizeâ€Transformable Nanostructures: From Design to Biomedical Applications. Advanced Materials, 2020, 32, e2003752.	21.0	52
46	Removing the barrier to water dissociation on single-atom Pt sites decorated with a CoP mesoporous nanosheet array to achieve improved hydrogen evolution. Journal of Materials Chemistry A, 2020, 8, 11246-11254.	10.3	62
47	Highâ€Performance Overall CO <sub>2</sub> Splitting on Hierarchical Structured Cobalt Disulfide with Partially Removed Sulfur Edges. Advanced Functional Materials, 2020, 30, 2000154.	14.9	26
48	Slower Removing Ligands of Metal Organic Frameworks Enables Higher Electrocatalytic Performance of Derived Nanomaterials. Small, 2020, 16, e2002210.	10.0	47
49	Two dimensional ZIF-derived ultra-thin Cu–N/C nanosheets as high performance oxygen reduction electrocatalysts for high-performance Zn–air batteries. Nanoscale, 2020, 12, 14259-14266.	5.6	34
50	Synthesis of Ultrathin MoS <sub>2</sub> Nanosheets Embedded in 3D Hierarchically Nitrogenâ€andâ€5ulfur Coâ€Doped Porous Carbon Composites as Efficient Oxygen Reduction Reaction Catalyst. ChemElectroChem, 2020, 7, 3260-3268.	3.4	4
51	Novel Heteroatom-Doped Fe/N/C Electrocatalysts With Superior Activities for Oxygen Reduction Reaction in Both Acid and Alkaline Solutions. Frontiers in Chemistry, 2020, 8, 78.	3.6	10
52	Co <sub>3</sub> O <sub>4</sub> Hollow Porous Nanospheres with Oxygen Vacancies for Enhanced Li–O <sub>2</sub> Batteries. ACS Applied Energy Materials, 2020, 3, 4014-4022.	5.1	57
53	A CoO <sub>x</sub> /FeO <sub>x</sub> heterojunction on carbon nanotubes prepared by plasma-enhanced atomic layer deposition for the highly efficient electrocatalysis of oxygen evolution reactions. Journal of Materials Chemistry A, 2020, 8, 15140-15147.	10.3	27
54	Recent Progress in Selfâ€Supported Catalysts for CO <sub>2</sub> Electrochemical Reduction. Small Methods, 2020, 4, 1900826.	8.6	48

XIANGZHONG REN

#	Article	IF	CITATIONS
55	Carbon dioxide electroreduction on single-atom nickel decorated carbon membranes with industry compatible current densities. Nature Communications, 2020, 11, 593.	12.8	330
56	Construction of tetrahedral CoO <sub>4</sub> vacancies for activating the high oxygen evolution activity of Co <sub>3â^'x</sub> O <sub>4â^'Î</sub> porous nanosheet arrays. Nanoscale, 2020, 12, 11079-11087.	5.6	35
57	MoS <sub>2</sub> nanoflowers encapsulated into carbon nanofibers containing amorphous SnO <sub>2</sub> as an anode for lithium-ion batteries. Nanoscale, 2019, 11, 16253-16261.	5.6	52
58	Enhanced structural stability and overall conductivity of Li-rich layered oxide materials achieved by a dual electron/lithium-conducting coating strategy for high-performance lithium-ion batteries. Journal of Materials Chemistry A, 2019, 7, 23964-23972.	10.3	25
59	Heterostructured CoO-Co <sub>3</sub> O <sub>4</sub> nanoparticles anchored on nitrogen-doped hollow carbon spheres as cathode catalysts for Li–O <sub>2</sub> batteries. Nanoscale, 2019, 11, 14769-14776.	5.6	31
60	Free-Standing Selenium Impregnated Carbonized Leaf Cathodes for High-Performance Sodium-Selenium Batteries. Nanoscale Research Letters, 2019, 14, 30.	5.7	11
61	Rational design of positive-hexagon-shaped two-dimensional ZIF-derived materials as improved bifunctional oxygen electrocatalysts for use as long-lasting rechargeable Zn–Air batteries. Applied Catalysis B: Environmental, 2019, 256, 117871.	20.2	70
62	Ultra small few layer MoS2 embedded into three-dimensional macro-micro-mesoporous carbon as a high performance lithium ion batteries anode with superior lithium storage capacity. Electrochimica Acta, 2019, 317, 638-647.	5.2	43
63	Hierarchical CuO <sub>x</sub> –Co <sub>3</sub> O <sub>4</sub> heterostructure nanowires decorated on 3D porous nitrogen-doped carbon nanofibers as flexible and free-standing anodes for high-performance lithium-ion batteries. Journal of Materials Chemistry A, 2019, 7, 7691-7700.	10.3	90
64	A lithium carboxylate grafted dendrite-free polymer electrolyte for an all-solid-state lithium-ion battery. Journal of Materials Chemistry A, 2019, 7, 25818-25823.	10.3	21
65	Co-CoO/MnO Heterostructured Nanocrystals Anchored on N/P-Doped 3D Porous Graphene for High-Performance Pseudocapacitive Lithium Storage. Journal of the Electrochemical Society, 2019, 166, A3820-A3829.	2.9	9
66	Scalable 2D Hierarchical Porous Carbon Nanosheets for Flexible Supercapacitors with Ultrahigh Energy Density. Advanced Materials, 2018, 30, 1706054.	21.0	405
67	New Strategy for Polysulfide Protection Based on Atomic Layer Deposition of TiO <sub>2</sub> onto Ferroelectricâ€Encapsulated Cathode: Toward Ultrastable Freeâ€Standing Room Temperature Sodium–Sulfur Batteries. Advanced Functional Materials, 2018, 28, 1705537.	14.9	167
68	Enhanced electrocatalytic performance of Fe-TiO2/N-doped graphene cathodes for rechargeable Li-O2 batteries. Journal of Solid State Electrochemistry, 2018, 22, 909-917.	2.5	14
69	Flexible Three-Dimensional Heterostructured ZnO-Co <sub>3</sub> O <sub>4</sub> on Carbon Cloth as Free-Standing Anode with Outstanding Li/Na Storage Performance. Journal of the Electrochemical Society, 2018, 165, A3932-A3942.	2.9	32
70	PdNi alloy decorated 3D hierarchicallyÂN, S co-doped macro–mesoporous carbon composites as efficient free-standing and binder-free catalysts for Li–O <sub>2</sub> batteries. Journal of Materials Chemistry A, 2018, 6, 10856-10867.	10.3	47
71	Spinel photocatalysts for environmental remediation, hydrogen generation, CO <sub>2</sub> reduction and photoelectrochemical water splitting. Journal of Materials Chemistry A, 2018, 6, 11078-11104.	10.3	176
72	LiFePO <sub>4</sub> /RGO composites synthesized by a solid phase combined with carbothermal reduction method. Ferroelectrics, 2018, 528, 1-7.	0.6	7

XIANGZHONG REN

#	Article	IF	CITATIONS
73	The enhancement of electrochemical capacitance of biomass-carbon by pyrolysis of extracted nanofibers. Electrochimica Acta, 2017, 228, 398-406.	5.2	73
74	Facile synthesis of PdSnCo/nitrogen-doped reduced graphene as a highly active catalyst for lithium-air batteries. Electrochimica Acta, 2017, 228, 36-44.	5.2	31
75	Mesoporous NiCo <sub>2</sub> O <sub>4</sub> networks with enhanced performance as counter electrodes for dye-sensitized solar cells. Dalton Transactions, 2017, 46, 4403-4411.	3.3	26
76	CoO-Co 3 O 4 heterostructure nanoribbon/RGO sandwich-like composites as anode materials for high performance lithium-ion batteries. Electrochimica Acta, 2017, 241, 252-260.	5.2	69
77	Preparation and electrochemical properties of Si0.8Sb/C nanofiber composite anode materials for lithium-ion batteries. Journal of Solid State Electrochemistry, 2017, 21, 2281-2289.	2.5	7
78	Ternary PdNi-based nanocrystals supported on nitrogen-doped reduced graphene oxide as highly active electrocatalysts for the oxygen reduction reaction. Electrochimica Acta, 2017, 235, 543-552.	5.2	45
79	Atomic layer deposition of TiO2 on nitrogen-doped carbon nanofibers supported Ru nanoparticles for flexible Li-O2 battery: A combined DFT and experimental study. Journal of Power Sources, 2017, 368, 88-96.	7.8	19
80	One-step rapid in-situ synthesis of nitrogen and sulfur co-doped three-dimensional honeycomb-ordered carbon supported PdNi nanoparticles as efficient electrocatalyst for oxygen reduction reaction in alkaline solution. Electrochimica Acta, 2017, 253, 445-454.	5.2	20
81	Air plasma etching towards rich active sites in Fe/N-porous carbon for the oxygen reduction reaction with superior catalytic performance. Journal of Materials Chemistry A, 2017, 5, 16605-16610.	10.3	45
82	Electrospun NiCo2S4 with extraordinary electrocatalytic activity as counter electrodes for dye-sensitized solar cells. Journal of Solid State Electrochemistry, 2017, 21, 3579-3588.	2.5	15
83	Atomic layer deposition of amorphous oxygen-deficient TiO2-x on carbon nanotubes as cathode materials for lithium-air batteries. Journal of Power Sources, 2017, 360, 215-220.	7.8	34
84	Facile synthesis of N-doped carbon-coated Si/Cu alloy with enhanced cyclic performance for lithium ion batteries. RSC Advances, 2016, 6, 78100-78105.	3.6	6
85	Three-dimensional nanoarchitecture SnSbZn–C composite nanofibers as anode materials for lithium-ion batteries. RSC Advances, 2016, 6, 52746-52753.	3.6	5
86	Carbon-coated LiFePO4synthesized by a simple solvothermal method. CrystEngComm, 2016, 18, 7537-7543.	2.6	12
87	In situ growth of morphology-controllable nickel sulfides as efficient counter electrodes for dye-sensitized solar cells. Journal of Solid State Electrochemistry, 2016, 20, 2373-2382.	2.5	17
88	3D Networks of Carbonâ€Coated Magnesiumâ€Doped Olivine Nanofiber as Binderâ€Free Cathodes for Highâ€Performance Liâ€Ion Battery. Advanced Materials Interfaces, 2016, 3, 1600241.	3.7	14
89	Preparation and electrochemical performance of Cu6Sn5/CNTs anode materials for lithium-ion batteries. Integrated Ferroelectrics, 2016, 171, 193-202.	0.7	3
90	Synthesis of Si-Sb-ZnO Composites as High-Performance Anodes for Lithium-ion Batteries. Nanoscale Research Letters, 2015, 10, 414.	5.7	12

#	Article	IF	CITATIONS
91	SnSb–ZnO composite materials as high performance anodes for lithium-ion batteries. RSC Advances, 2015, 5, 105643-105650.	3.6	11